PROCEEDINGS OF SCIENCE

Cosmic-Ray Transport under the Influence of Non-linear Landau Damping

Benedikt Schroer ,[a,*] **Damiano Caprioli** [a,b] **and Pasquale Blasi** [c,d]

[a] *Department of Astronomy and Astrophysics, University of Chicago, 5640 S Ellis Ave, Chicago, IL 60637, USA*

[b] *Enrico Fermi Institute, The University of Chicago, Chicago, IL 60637, USA*

[c] *Gran Sasso Science Institute (GSSI), Viale Francesco Crispi 7, 67100 L'Aquila, Italy*

[d] *INFN-Laboratori Nazionali del Gran Sasso (LNGS), via G. Acitelli 22, 67100 Assergi (AQ), Italy*

E-mail: bschroer@uchicago.edu

We present the first investigation of the role of non-linear Landau damping in self-generated cosmic-ray transport in conditions appropriate for the Galactic halo using hybrid particle-in-cell simulations. We find reduced CR drift speeds due to scattering, that however, remain super-Alfvénic due to damping. The non-linear Landau damping leads to heating of the background plasma and initiates an inverse cascade, producing perturbations on non-resonant large scales, a result with many potential implications for CR transport.

39th International Cosmic Ray Conference (ICRC2025)
15–24 July 2025
Geneva, Switzerland

[*] Speaker

PoS(ICRC2025)128

1. Introduction

Modeling cosmic-ray (CR) transport requires understanding the interplay between various physical processes, especially the role of turbulent magnetic fields. Observations of secondary-to-primary CR ratios [1, 2, 9] indicate that CRs diffuse by scattering on these turbulent fields, but whether such turbulence is self-generated by CRs or injected at large scales (e.g., by supernovae) remains debated. The recently observed spectral breaks in these ratios may signal CR-driven excitation of streaming instabilities [5, 8, 11], while pre-existing turbulence potentially becomes relevant at energies $\gtrsim$ TeV.

CR transport involving streaming instabilities is inherently non-linear, as the instability growth rate depends on the CR distribution, and thus on the propagation itself. On Galactic scales, the resonant streaming instability is a likely mechanism for CR confinement up to at least TeV energies [5, 7, 11]. However, the efficiency of self-confinement critically depends on damping processes that saturate instability growth and thus dictate the energy dependence of the diffusion coefficient.

If streaming instability growth outweighs damping, CRs isotropize and their drift speed v_D reduces to the Alfvén velocity v_A. At higher energies, though, the energy-dependent decrease in secondary-to-primary ratios implies particles increasingly drift super-Alfvénically ($v_D > v_A$), consistent with wave growth being limited by damping [17]. In different interstellar phases, this can be driven by ion-neutral damping [17], non-linear Landau damping (NLLD) [18], or other mechanisms [6, 14, 15, 19]. In hot ionized media, where neutrals are negligible, NLLD is dominant both on Galactic scales [18] and near sources [10, 20, 21].

NLLD acts through Alfvén wave interactions, transferring wave energy to the plasma as heat [18]. For a turbulent spectrum, wave growth or damping depends on interactions with all other waves—a point often neglected in earlier work [3, 10, 21, 26, 27]. If both wave polarizations are balanced, damping dominates; but with a slight excess in one polarization, energy can cascade to larger scales, possibly driving an inverse cascade [16].

Most prior studies of streaming instability's saturation focused on the $\beta \ll 1$ regime or on ion-neutral damping and used PIC or MHD-PIC methods [4, 13, 22]. Yet, these works do not address the hot ionized phase where NLLD is dominant and CRs spend most of their lifetime.

Here, we investigate the saturation of the resonant streaming instability in the astrophysically relevant regime $\beta \gtrsim 1$ using hybrid PIC simulations. We present the first direct evidence that NLLD operates in such plasma, leading to reduced CR drift, and we continuously inject CRs to mimic realistic Galactic conditions. Our results show that wave modes of a given scale are damped by all longer scales present and reveal a small CR-induced polarization excess, driving an inverse cascade as discussed above.

The paper is structured as follows: Section 2 details our simulation setup, Section 3 presents our findings, and Section 5 concludes.

2. PIC simulations

We study particle self-confinement in the presence of NLLD with dHybridR a relativistic hybrid code with kinetic ions and (massless, charge-neutralizing) fluid electrons [12]. In our simulations, lengths, time, velocities, number densities and magnetic fields are normalized to the ion inertial

length $d_i = v_A/\Omega_{ci}$, the inverse ion cyclotron frequency Ω_{ci}^{-1}, v_A, the number density (n_0) and the magnetic field strength (B_0) of the initial background plasma respectively. The background ions are thermal ions with gyroradius $r_{g,i} = d_i$, i.e. $\beta_i = 2v_{th,i}^2/v_A^2 = 2$ and 128 particles per cell. The simulation box is filled with a background magnetic field along the x-direction with a strength B_0.

Our simulations are quasi-1D along x and all three components of the momenta and electromagnetic fields are retained. The box is $60000\, d_i \times 5\, d_i$ large, divided into 120000×10 cells. Our time step is set to $0.005\, \Omega_{ci}^{-1}$ and the speed of light $c = 100\, v_A$. The boundary conditions are the following: periodic for the background plasma, periodic in y and open in x for the CRs and the magnetic fields. CRs are injected with 16 particles per cell with a distribution that is isotropic in a CR rest frame and then boosted with p_{bst} into the simulation frame. They have an isotropic momentum $p_{iso} = 100\, mv_A$ (Lorentz factor $\sqrt{2}$), drift speed $v_D = 4\, v_A$ and $n_{CR} = 2 \times 10^{-5}\, n_0$. We perform a second simulation with an additional CR species with $p_{iso} = 300\, mv_A$ and $n_{CR} = 2 \times 10^{-5}\, n_0$ and $v_D = 12\, v_A$ and a three times larger box along x keeping two cells per d_i.

3. Results

3.1 Non-Linear Landau Damping

In Fig. 1, we show the power spectrum of the turbulent magnetic field as a function of wave number k at different points in time for simulation I. Initially, the resonant streaming instability is excited, which grows the field on resonant scales ($\lesssim r_L = 100, d_i$), corresponding to the blue lines in the figure. Around $\sim 17\gamma_{max}^{-1}$ (light blue), the field saturates on resonant scales, while at the same time it starts growing on scales $\gtrsim r_L$. After saturation, an inverse cascade removes power from small scales and shifts it toward larger scales, as is evident from Fig. 1. The inverse cascade can be interpreted as a feature of NLLD. In the linear analysis [18], when two waves of the same polarization interact, the large-wavelength wave gains energy, while the small-wavelength wave is damped. For a linearly polarized wave spectrum, this growth of large-scale modes naively would cancel out exactly due to interactions with opposite polarized waves. However, in our simulation and arguably in the Galaxy, the small CR anisotropy introduces a slight imbalance of polarizations that kickstarts the inverse cascade.

Contrary to common approximations [21, 23, 24, 26], it can be seen that smaller wavelength modes suffer stronger damping losses, consistent with the assessment of early works [25] that the damping rate at a given scale depends on the integral over all power on longer scales. Once the inverse cascade starts, power is removed from small scales and shifted towards large scales that are not resonant with any particles in our simulation. These waves continue to grow until a balance is reached between their growth and the waves that are leaving the box.

3.2 Evolution of the Magnetic Field and CR Drift Speed

The overall evolution of the CR drift speed and the magnetic field in simulation I is illustrated in Fig. 2. Four different phases can be identified, each with a unique interplay of CRs and fields. During the free streaming phase, CRs are not affected by the presence of magnetic fields and excite the resonant instability with a growth rate that can be derived from [16]. Around $t = 3\, \gamma_{max}^{-1}$, resonant scattering becomes effective inside the box. At this point $\delta B^2/B_0^2 \gtrsim 10^{-3}$, resulting in a

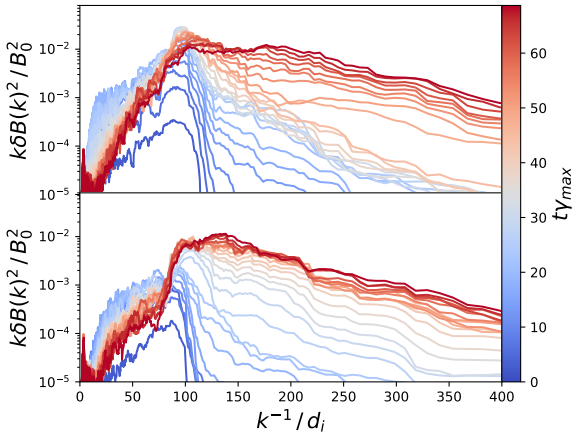

Figure 1: Power spectra of the magnetic field $\delta B_y \mp i\delta B_z$at different k for left-handed (top panel) and right-handed (bottom panel) modes, respectively. Small-scale power is transferred to large scales, indicating an inverse cascade.

mean free path $\lambda \approx \frac{\mu c}{\Omega} \frac{2B_0^2}{\pi k_{res}\delta B(k_{res})^2}$ smaller than the length of our box with the pitchangle μ and the resonant wave number $k_{res} = 1/(\mu r_L)$. As a result, CRs start to diffuse and collectively slow down. The scattering redistributes the particles in phase space, changing the growth rate of the instability in the process.

The turbulent field keeps growing until $\sim 17\gamma_{max}^{-1}$, when its growth is balanced by damping processes, see previous section. From this point onward, the magnetic field at resonant scales (orange line) stalls and is damped away, while the field on large scales keeps increasing. This redistribution of the field is a result of an inverse cascade in k-space that moves power to increasingly larger scales. Removing power from small scales makes it increasingly difficult to scatter particles with small pitchangles and to cross the 90° barrier in pitchangle, reducing the efficacy of resonant scattering and leading to an increasing drift speed due to less efficient diffusion.

After $t \approx 60\,\gamma_{max}^{-1}$, the total field and the drift speed flatten out, indicating saturation and a final steady state. At this point, a balance is reached between waves leaving the box via the open boundary and new waves being created by the inverse cascade. The balance critically depends on the growth rate of the nonresonant fields. The growth rate in the linear analysis, is proportional to the total power on scales smaller than the scale of interest. Hence, roughly one Alfvén-passing time $L/v_A \sim 26\,\gamma_{max}^{-1}$ after the power on resonant scales peaked, we see the power on nonresonant scales saturating.

4. Simulation II

The appearance of long wavelength waves from the self-generation of the resonant streaming instability of low energy CRs is a point of major interest since in models of Galactic CR transport, large-scale turbulence is typically assumed to be extrinsic caused by supernova explosions [5, 11] or produced by high-energy CRs in resonance with these scales [8]. Instead, the inverse cascade provides a way for low-energy CRs to grow turbulence on these large scales.

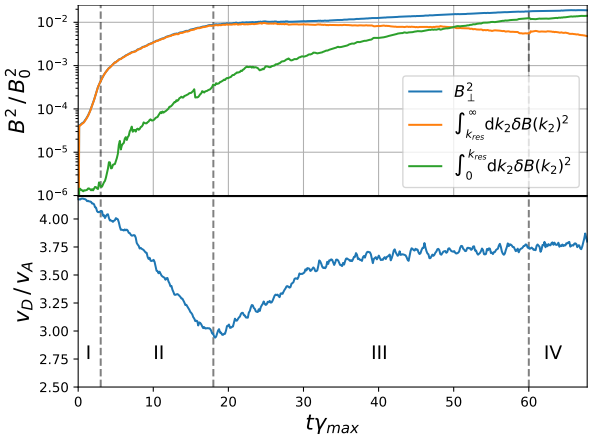

Figure 2: Bottom panel: Box averaged CR drift velocity as a function of time. Top panel: Magnetic field on all scales smaller than r_L (orange), larger than r_L (green) and total perpendicular (blue) as a function of time. Time is in units of γ_{max}. Dashed lines indicate the transition of different evolutionary stages.

To investigate a possible impact on higher energy particles, we perform a second simulation with an additional high-energy CR population. In Fig. 3, we show the magnetic field, split into total field and fields resonant and nonresonant with low-energy CRs and drift speed of the two CR populations normalized to their initial drift speed. The first thing to note is that the green line includes scales that are still resonant with CRs of population II. Hence, the large-scale fields grow faster than before due to the resonant streaming instability excited by high-energy CRs. As a result, the large-scale fields dominate much earlier compared to the previous case. Even more importantly: Due to the fields excited by high-energy CRs, the small-scale fields saturate at a lower value compared with the case with only one CR population because damping becomes significant much earlier. As a result, the damping of small-scale modes is more severe throughout the simulation and the total power on small-scales falls off by a factor of 3.

Interestingly, the drift speed reached by population I is comparable with the previous simulation, since the fields reach comparable levels. This confirms, that our previous box is sufficiently large to fully capture the resonant scattering of this population. Instead, the drift speed of the high-energy CRs is influenced by scattering off the fields generated by low-energy particles. The enhanced scattering is mainly due to high-energy CRs with small pitch angles $\mu \leq 0.3$ that are in resonance with these fields. Unfortunately, we cannot determine the impact of the inverse cascade on population II, as the numerical limitations prevent a sufficient scale separation of energies that would be necessary for this. At late times, the inverse cascade again populates scales that are not in resonance with any particles, while the resonant fields are damped and their power slowly decreases. All these considerations are in agreement with expectations based on the results inferred from our previous one-CR simulation.

5. Conclusions

We discuss the role of NLLD in saturating the resonant streaming instability in a high-β plasma. While, in the absence of this damping, it is expected that CRs would excite Alfvén waves until they

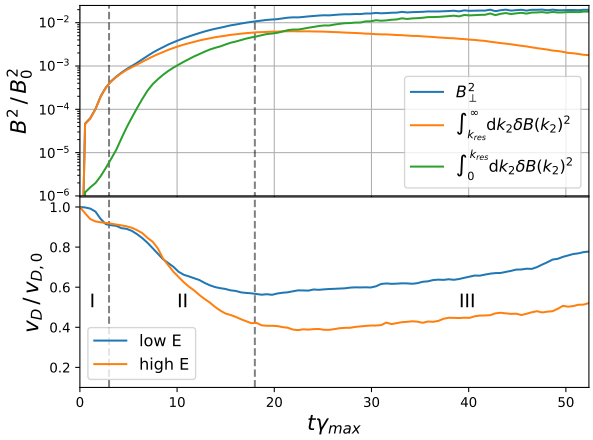

Figure 3: Same as Fig. 2, but for a simulation with an additional high-energy CR population. The separation of orange and green line is the same as before meaning k_{res} corresponds to the gyroradius of the low energy CR particles.

fully isotropize in the wave frame, CRs can maintain an energy-dependent drift speed when damping is present. In the Galactic halo, it was shown that this process can lead to the self-generation of a CR halo [5, 8, 11] and explain CR fluxes at Earth.

Here, we test the role of NLLD with hybrid-PIC simulations of a periodic box in which a slowly drifting CR distribution excites Alfvén waves that are able to leave the system, mimicking a fluid element close to the Galactic disk. We confirm a super-alfvénic drift speed at saturation of the instability. Furthermore, we find that damping at a given scale occurs due to power on larger scales, in accordance with early linear analysis of the phenomenon [18, 25], but opposing commonly used approximations [3, 10, 21, 26, 27]. As a result, small-scale modes suffer the strongest damping which leads to the development of a pitch angle barrier. Additionally, we find that an inverse cascade develops, that moves power from small to large scales which might have profound implications for CR transport on Galactic scales.

To further test our conclusions, we performed a second simulation with an additional CR population with higher energy. The behavior of the fields and CRs in the second simulation is consistent with the findings of the first simulation. The additional CR population creates more fields on large scales due to the resonant streaming instability which leads to a saturation at a lower magnetic field on resonant scales and stronger damping. As before, the inverse cascade grows fields on scales larger than the resonant scale of any particle in the simulation.

Acknowledgments

Simulations were performed on computational resources provided by the University of Chicago Research Computing Center and on TACC's Stampede3 through ACCESS Maximize allocation PHY240042.

This work of D.C. was partially supported by NASA through grants 80NSSC18K1218 and 80NSSC24K0173 and NSF through grants PHY-2010240, and AST-2009326. The work of P.B.

was partially supported by the European Union – NextGenerationEU RRF M4C2 1.1 under grant PRIN-MUR 2022TJW4EJ.

References

[1] O. Adriani et al. [CALET Collaboration]. Cosmic-Ray Boron Flux Measured from 8.4 GeV /n to 3.8 TeV /n with the Calorimetric Electron Telescope on the International Space Station. , 129(25):251103, Dec. 2022.

[2] M. Aguilar et al. [AMS Collaboration]. The Alpha Magnetic Spectrometer (AMS) on the international space station: Part II - Results from the first seven years. *Phys. Rep.*, 894:1–116, Feb. 2021.

[3] L. Armillotta, E. C. Ostriker, and Y.-F. Jiang. Cosmic-Ray Transport in Simulations of Star-forming Galactic Disks. , 922(1):11, Nov. 2021.

[4] X.-N. Bai, E. C. Ostriker, I. Plotnikov, and J. M. Stone. Magnetohydrodynamic Particle-in-cell Simulations of the Cosmic-Ray Streaming Instability: Linear Growth and Quasi-linear Evolution. , 876(1):60, May 2019.

[5] P. Blasi, E. Amato, and P. D. Serpico. Spectral breaks as a signature of cosmic ray induced turbulence in the galaxy. *Physical Review Letters*, 109(6):061101, Aug. 2012.

[6] S. S. Cerri. Revisiting the role of cosmic-ray driven Alfvén waves in pre-existing magnetohydrodynamic turbulence. I. Turbulent damping rates and feedback on background fluctuations. *arXiv e-prints*, page arXiv:2402.02901, Feb. 2024.

[7] D. O. Chernyshov, V. A. Dogiel, A. V. Ivlev, A. D. Erlykin, and A. M. Kiselev. Formation of the Cosmic-Ray Halo: The Role of Nonlinear Landau Damping. , 937(2):107, Oct. 2022.

[8] D. O. Chernyshov, A. V. Ivlev, and V. A. Dogiel. Secondary cosmic-ray nuclei in the Galactic halo model with nonlinear Landau damping. *A&A*, 686:A165, June 2024.

[9] Dampe Collaboration. Detection of spectral hardenings in cosmic-ray boron-to-carbon and boron-to-oxygen flux ratios with DAMPE. *Science Bulletin*, 67(21):2162–2166, Nov. 2022.

[10] M. D'Angelo, P. Blasi, and E. Amato. Grammage of cosmic rays around Galactic supernova remnants. , 94(8):083003, Oct. 2016.

[11] C. Evoli, P. Blasi, G. Morlino, and R. Aloisio. Origin of the Cosmic Ray Galactic Halo Driven by Advected Turbulence and Self-Generated Waves. , 121(2):021102, July 2018.

[12] C. C. Haggerty and D. Caprioli. dHybridR: A Hybrid Particle-in-cell Code Including Relativistic Ion Dynamics. , 887(2):165, 12 2019.

[13] C. Holcomb and A. Spitkovsky. On the Growth and Saturation of the Gyroresonant Streaming Instabilities. , 882(1):3, Sept. 2019.

[14] P. F. Hopkins, J. Squire, I. S. Butsky, and S. Ji. Standard self-confinement and extrinsic turbulence models for cosmic ray transport are fundamentally incompatible with observations. *MNRAS*, 517(4):5413–5448, Dec. 2022.

[15] P. F. Hopkins, J. Squire, T. K. Chan, E. Quataert, S. Ji, D. Kereš, and C.-A. Faucher-Giguère. Testing physical models for cosmic ray transport coefficients on galactic scales: self-confinement and extrinsic turbulence at ∼GeV energies. *MNRAS*, 501(3):4184–4213, Mar. 2021.

[16] R. Kulsrud and W. P. Pearce. The effect of wave-particle interactions on the propagation of cosmic rays. , 156:445, May 1969.

[17] R. M. Kulsrud and C. J. Cesarsky. The Effectiveness of Instabilities for the Confinement of High Energy Cosmic Rays in the Galactic Disk. *ApJL*, 8:189, Mar. 1971.

[18] M. A. Lee and H. J. Völk. Damping and Non-Linear Wave-Particle Interactions of Alfvén-Waves in the Solar Wind. *ApSS*, 24(1):31–49, Sept. 1973.

[19] R. Lemmerz, M. Shalaby, C. Pfrommer, and T. Thomas. The theory of resonant cosmic ray-driven instabilities – Growth and saturation of single modes. *arXiv e-prints*, page arXiv:2406.04400, June 2024.

[20] L. Nava, S. Gabici, A. Marcowith, G. Morlino, and V. S. Ptuskin. Non-linear diffusion of cosmic rays escaping from supernova remnants - i. the effect of neutrals. *MNRAS*, 461:3552–3562, Oct. 2016.

[21] L. Nava, S. Recchia, S. Gabici, A. Marcowith, L. Brahimi, and V. Ptuskin. Non-linear diffusion of cosmic rays escaping from supernova remnants - II. Hot ionized media. *MNRAS*, 484(2):2684–2691, Apr. 2019.

[22] I. Plotnikov, E. C. Ostriker, and X.-N. Bai. Influence of Ion-Neutral Damping on the Cosmic-Ray Streaming Instability: Magnetohydrodynamic Particle-in-cell Simulations. , 914(1):3, June 2021.

[23] S. Recchia, P. Blasi, and G. Morlino. Cosmic ray driven galactic winds. *MNRAS*, 462:4227–4239, Nov. 2016.

[24] S. Recchia, D. Galli, L. Nava, M. Padovani, S. Gabici, A. Marcowith, V. Ptuskin, and G. Morlino. Grammage of cosmic rays in the proximity of supernova remnants embedded in a partially ionized medium. *A&A*, 660:A57, Apr. 2022.

[25] H. J. Völk and C. J. Cesarsky. Nonlinear Landau damping of Alfvén waves in a high beta plasma. *Zeitschrift Naturforschung Teil A*, 37:809–815, Jan. 1982.

[26] J. Wiener, E. G. Zweibel, and S. P. Oh. Cosmic Ray Heating of the Warm Ionized Medium. , 767(1):87, Apr. 2013.

[27] J. Wiener, E. G. Zweibel, and S. P. Oh. High β effects on cosmic ray streaming in galaxy clusters. *MNRAS*, 473(3):3095–3103, Jan. 2018.